Appl. Phys. B 60, 169–179 (1995)

Applied Physics B Lasers and Optics

A wire trap for neutral atoms

J. Schmiedmayer[1–3]

[1] Institut für Experimentalphysik, Universität Innsbruck, Technikerstrasse 25, A-6020 Innsbruck, Austria
(Fax: + 43-512/507-2921, E-mail: Joerg. Schmiedmayer @uibk.ac.at)
[2] Rowland Institute of Science, Cambridge, MA, USA
[3] Department of Physics, Harvard University, Cambridge, MA, USA

Received: 15 September 1994/Accepted: 2 November 1994

Abstract. We present new ways of trapping a neutral atom with static electric and magnetic fields. We discuss the interaction of a neutral atom with the magnetic field of a current carrying wire and the electric field of a charged wire. Atoms can be trapped by the $1/r$ magnetic field of a current-carrying wire in a two-dimensional trap. The atoms move in Kepler-like orbits around the wire and angular momentum prevents them from being absorbed at the wire. Trapping was demonstrated in an experiment by guiding atoms along a 1 m long current-carrying wire. Stable traps using the interaction of a polarizable atom with the electric field of a charged wire alone are not possible because of the $1/r^2$ form of the interaction potential. Nevertheless, we show that one can build a microscopic trap with a combination of a magnetic field generated by a current in a straight wire and the static electric field generated by a concentric charged ring which provides the longitudinal confinement. In all of these traps, the neutral atoms are trapped in a region of maximal field, in their *high-field seeking* state.

PACS: 52.55.Lf; 32.80.Pj; 83.75.Bc

In the last decades, electromagnetic traps for ions have been developed and used for a large number of pioneering experiments [1]. Trapping neutral atoms is more difficult, since their interactions with magnetic and electric fields are much weaker. The interaction potentials of neutral atoms with static fields are: $V_{\text{mag}} = -\boldsymbol{\mu}\cdot\mathbf{B}$ due to the magnetic moment of the atom in a magnetic field, and $V_{\text{pol}} = -\alpha E^2/2$ for the interaction stemming from the electric polarizability of the atom in an electric field. Realizable traps are very shallow, generally less than 1 K deep.

Recently, the development of new techniques to cool and slow neutral atoms to low velocities [2] has made trapping of neutral particles in static magnetic fields possible [3]. Neutrons [4], hydrogen [5], and alkali atoms [6] have been trapped in magnetic storage rings, bottles, and traps. In all of these experiments, the particles were trapped in a local *minimum* of the magnetic field, in a so called "*low-field seeking state*". In these traps, the magnetic moment is anti-parallel to the magnetic field, i.e., $V_{\text{mag}} > 0$; therefore, the atoms are trapped in an exited state of the particle–field system. The stored potential energy, which is always larger than the trap depth, can be released by bipolar spin relaxation to the ground state in binary collisions [7]. The particle will leave the trap.

The ideal magnetic trap would have a magnetic-field maximum that captures atoms in a "*high-field seeking state*". This high-field seeking state has the magnetic moment parallel to the magnetic field, i.e., $V_{\text{mag}} < 0$; hence, the particle–field system is in its ground state. In these traps, energy conservation prohibits the two-body spin-flip process, and the trap will be more stable at high densities. Traps based on the interaction of a neutral atom with the electric field ($V_{\text{pol}} = -\alpha E^2/2$) are always "*high-field seeker*" traps.

However, the classical Earnshaw theorem forbids the creation of a local maximum of the magnetic field in free space [8]. It was shown that the same holds true for any combination of electric, magnetic, and gravitational fields [9].

The above restrictions can be circumvented if the source of the field lies inside the trapping region. A maximum of the magnetic field can be found in a region of non-zero current which can be created by a current-carrying wire [10]. A maximum of the electric field and, therefore, a minimum of the interaction potential between the field and a polarizable atom can be found in a region of non-zero charge density. Such a geometry can be achieved by a charged wire or a well-defined beam of charged particles. In these field configurations, the atoms would be trapped in the lowest particle-field state.

To sustain a stable trap, the atom has to be kept away from the wire, because atoms generally are absorbed at surfaces. This can be achieved by the potential barrier created by the angular momentum L. In cylindrical

Dedicated to H. Walther on the occasion of his 60th birthday

geometry, the centripetal potential $V_l = L^2/2Mr^2$ can compensate for all regular potentials which diverge less rapidly than r^{-2} as $r \to 0$.

In the remainder of the paper, we will focus on various possibilities of trapping a neutral atom with a wire. In Sect. 1, we discuss the interaction between a neutral atom possessing a magnetic moment and a current-carrying wire. We will show that atoms can orbit the wire in Kepler-like orbits in the regime of classical physics. We also present a novel experiment which demonstrates two-dimensional trapping of an atom on a wire. In Sect. 2, we will investigate the interaction of a charged wire with a polarizable atom. Even though trapping with a static electric potential alone is impossible, the electric interaction can be used in combination with the magnetic interaction to form a three-dimensional trap for neutral atoms, as shown in Sect. 3.

1 Atom and a current

Consider a neutral atom with mass M and magnetic moment μ placed at distance r from the center of a straight wire with current I flowing through it (Fig. 1). The magnetic field at the distance r from the wire is given by (in Gaussian units):

$$\mathbf{B}(r) = \frac{2}{c} I \times \hat{\mathbf{e}}_r \frac{1}{r}. \tag{1}$$

$\hat{\mathbf{e}}_r$ is the unit vector in the radial direction. The atom interacts with the magnetic field of the current-carrying wire by the potential $V = -\boldsymbol{\mu}\cdot\mathbf{B}$. The Hamiltonian for the motion of the atom in the magnetic field of a current-carrying wire is then given by:

$$H = \frac{P^2}{2M} - \boldsymbol{\mu}\cdot\mathbf{B}(r). \tag{2}$$

If the wire is straight, the motion along the wire is free and the problem reduces to two dimensions. From now on, we will focus only on the transverse motion. Assuming the current flows in the z-direction, the magnetic interaction

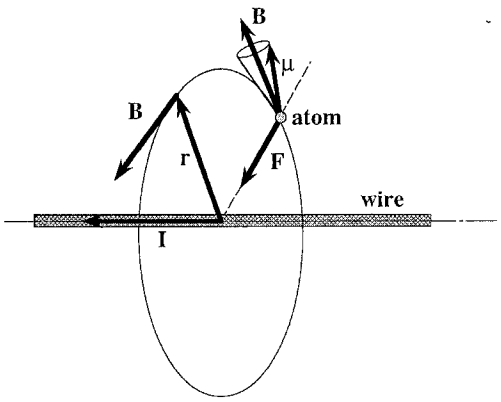

Fig. 1. Schematic of the interaction of a neutral atom possessing magnetic moment $\boldsymbol{\mu}$ with the magnetic field $\mathbf{B}$ of a wire carrying a current I

in H can be written as:

$$V_{\text{mag}}(\mathbf{r}) = -\frac{2I}{c}\frac{1}{r}\mu\cdot\hat{\mathbf{e}}_\varphi, \tag{3}$$

where $\hat{\mathbf{e}}_\varphi = -\hat{\mathbf{e}}_x \sin\varphi + \hat{\mathbf{e}}_y \cos\varphi$ is the unit vector in the φ direction around the wire. For a magnetic moment $\boldsymbol{\mu}$ parallel to the magnetic field, the interaction potential $V = -\boldsymbol{\mu}\cdot\mathbf{B}$ is attractive towards the wire, and binding is possible.

1.1 Classical motion

Let us first consider the classical motion of the atom around the wire. The dynamics of a point particle with a magnetic moment in an arbitrary magnetic field is given by the equations of motion:

$$M\frac{\mathrm{d}^2}{\mathrm{d}t^2}\mathbf{x} = -\nabla[\boldsymbol{\mu}\cdot\mathbf{B}(\mathbf{x})], \tag{4a}$$

$$\frac{\hbar}{\gamma}\frac{\mathrm{d}}{\mathrm{d}t}\boldsymbol{\mu} = \boldsymbol{\mu}\times\mathbf{B}(\mathbf{x}). \tag{4b}$$

Here, $\mathbf{x}$ is the position of the atom and M its mass and $\gamma = g_F\mu_B$ is the gyro magnetic ratio of the atom. Equation (4a) describes the spatial part of the motion. It is complicated by the fact that the potential depends on the dot product of the two vectors $\boldsymbol{\mu}$ and $\mathbf{B}$. The force, therefore, depends on the relative orientation of the magnetic moment and the magnetic field. The motion of the magnetic-moment orientation is given by (4b). In general, $\boldsymbol{\mu}$ will precess around the direction of $\mathbf{B}$.

1.1.1 Adiabatic approximation. Moving in a classical trajectory around the wire, the atom will encounter a magnetic field changing in direction and strength. If the magnetic field varies slow enough, i.e., the precession of the magnetic moment is faster than the effective rotation of the magnetic field, one can apply an adiabatic approximation with the following familiar results [11, 12].

One can split the motion of the atom with the magnetic moment in two parts. One is a *fast motion* governing the spin precession of the magnetic moment, i.e., the internal degrees of freedom. The other is a *slow motion* of the atom around the wire, i.e., the external degrees of freedom. Employing the adiabatic approximation the external motion can be characterized by $\mu_\parallel = \boldsymbol{\mu}\cdot\mathbf{B}/|\mathbf{B}|$, the component of $\boldsymbol{\mu}$ parallel to the magnetic field. For a particle with spin $\mathbf{F}$, we have to treat this interaction, the spin motion, quantum mechanically. $\mu_\parallel$ is then given by $\mu_\parallel = \gamma m_F$, where m_F is the projection of $\mathbf{F}$ on the magnetic-field direction. $\mu_\parallel$ and m_F are adiabatic invariants, i.e., they are not changed by the slow motion [13].

The effective Hamiltonian that governs the external motion of the particle, the slow degrees of freedom, can be found using the full Born-Oppenheimer approximation. It includes a geometric vector potential $\mathbf{A}_{\text{adiabat}}$ and a scalar potential Φ_{adiabat} induced by the spatial variation of the magnetic-field direction $\hat{\mathbf{b}} = \mathbf{B}/|\mathbf{B}|$ [11, 12]. For the system of a neutral atom moving in the magnetic field of

a current-carrying wire we find:

$$H_{\text{eff}} = \frac{(\mathbf{P} - \mathbf{A}_{\text{adiabat}})^2}{2M} + \mathbf{\Phi}_{\text{adiabat}} - \frac{2I}{c\,r}\gamma m_F, \tag{5}$$

where the vector potential $\mathbf{A}_{\text{adiabat}}$ and the scalar potential $\mathbf{\Phi}_{\text{adiabat}}$ are given by:

$$\mathbf{A}_{\text{adiabat}} = \frac{m_F}{r}\hat{\mathbf{e}}_\varphi$$

$$\mathbf{\Phi}_{\text{adiabat}} = \frac{\hbar^2[F(F+1) - m_F^2]}{4M}\frac{1}{r^2}. \tag{6}$$

The vector potential $\mathbf{A}_{\text{adiabat}}$ itself does not result in a classical force, but will be important in the quantum-mechanical treatment. The scalar potential $\mathbf{\Phi}_{\text{adiabat}}$ gives a small repulsive $1/r^2$ interaction, repelling the classical motion from regions of non-adiabaticity. In this adiabatic approximation, we can separate (4a) governing the slow center-of-mass motion from (4b) governing the fast internal motion. The classical equations of motion in cylindrical coordinates can thus be simplified to:

$$M\frac{d^2}{dt^2}r = -\frac{d}{dr}\left[\frac{1}{r^2}\left(\frac{L^2}{2M} + \frac{\hbar^2[F(F+1) - m_F^2]}{4M}\right) - \frac{1}{r}\frac{2I}{c}\gamma m_F\right], \tag{7}$$

$$\frac{d}{dt}\varphi = \frac{L}{Mr^2}.$$

The resulting interaction potential governing the slow evolution is $V_{\text{mag}} = -\gamma|\mathbf{B}(\mathbf{r})|m_F$, which is a scalar. This potential is Coulomb-like $(1/r)$ [14] and, therefore, the atoms will circle the wire in Kepler-like orbits. The additional vector potential $\mathbf{A}$ has no effect on the classical motion, but will contribute a geometric phase which will be discussed in the quantum-mechanical treatment. The scalar potential $\mathbf{\Phi}$ has the form of $1/r^2$ and its effect will be an additional rotation of the orbit $\delta\varphi = -2\pi[F(F+1) - m_F^2]/4l^2$, where $\hbar l = L$ is the orbital angular momentum [15]. The orbits will not be closed. However, for $l \gg F$, the contribution of $\mathbf{\Phi}$ is very small and we can further simplify the adiabatic approximation by neglecting this term.

The adiabatic approximation holds when the Larmor precession $\omega_L = \gamma/\hbar \cdot B$ of the magnetic moment is much faster than the apparent rotation of the magnetic field ω_B in the rest frame of the moving atom ($\omega_L \gg \omega_B$). To test the range of parameters where the motion is adiabatic, we use a self-consistency argument. We assume that the motion is adiabatic and calculate the ratio ω_L/ω_B for orbits around the wire. Assuming a circular orbit for simplicity, the rotation of the magnetic-field direction is identical to the orbit frequency ω_o:

$$\omega_o = \frac{L}{M}\frac{1}{r^2} = \frac{4I^2}{c^2}\frac{\gamma^2 m_F^2}{L^3}, \tag{8}$$

where L is the angular momentum of the orbit, whereas the Larmor precession frequency ω_L is given by:

$$\omega_L = \frac{\gamma}{\hbar}B = \frac{4I^2}{c^2}\frac{\gamma^2 m_F}{\hbar L^2}. \tag{9}$$

For an atom in a circular orbit around a current-carrying wire, one finds from (8) and (9) that the ratio ω_L/ω_B is independent of mass M or current I: $\omega_L/\omega_B = \omega_L/\omega_o = L/\hbar m_F = l/m_F$. Therefore, for $l \gg 1$, the *adiabatic* approximation is valid and the atom will move in Kepler-like orbits. This classical motion, in the adiabatic approximation, is a nice example of "microscopic celestial mechanics" [16].

The basic relations between current, orbit radius, binding energy, and orbit frequency for circular orbits of a neutral atom with mass number A around a current-carrying wire are summarized in Table 1.

We can also determine when the adiabatic approximation is valid by integrating the full set of (4) to find the classical trajectories. In Fig. 2, we show trajectories calculated with initial conditions that would give circular orbits in the adiabatic approximation but with different degrees of adiabaticity given by the ratio ω_L/ω_O. One can easily see that for growing ω_L/ω_O, the orbits get more and more circular. For $\omega_L/\omega_O = 16$, the trajectory is very close to a circular orbit which would be expected in the adiabatic approximation.

1.2 Quantum motion

Let us now consider the quantum motion of a neutral atom with spin $\mathbf{F}$ in the magnetic field of a current $\mathbf{I}$. The

Table 1. Basic relations for trapping a neutral atom with mass number A and magnetic moment $g\mu_B$ in circular orbits around a current-carrying wire. The orbits are determined by two of the following parameters: current I, binding energy E_b, orbit radius r, and orbital angular momentum quantum number l

Current	Binding energy	Radius	l	ω_{Orbit}
I	$-1.603\dfrac{AI^2\mu^2}{l^2}$	$3.611\times10^{-6}\dfrac{l^2}{A\mu I}$	l	$4.870\times10^{15}\dfrac{A\mu I}{l^3}$
I	$-5.788\times10^{-6}\dfrac{\mu I}{r}$	r	$526.237\sqrt{A\mu Ir}$	$3.342\times10^{7}\sqrt{\dfrac{\mu I}{Ar^3}}$
I	E_b	$5.788\times10^{-6}\dfrac{\mu I}{E_b}$	$1.2660\,I\sqrt{\dfrac{A}{-E_b}}$	$2.400\times10^{15}\sqrt{\dfrac{-E_b^2}{A\mu I}}$
$\dfrac{0.0361\,l^2}{Ar\mu}$	$-0.00209\dfrac{l^2}{Ar^2}$	r	l	$6.35\times10^{12}\left(\dfrac{l}{Ar}\right)^2$

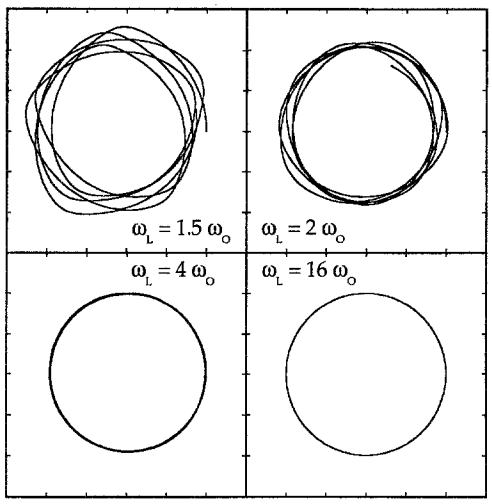

Fig. 2. Classical calculation of trajectories of a magnetic moment in the field of a current-carrying wire. The starting conditions were such that the adiabatic orbits would be circular. The trajectories are shown for various degrees of adiabaticity as given by the ratios ω_L/ω_O. For $\omega_L/\omega_O = 16$, the orbit is, on the scale of the drawing. indistinguishable from a circular Kepler orbit expected in the adiabatic limit

transverse motion is described by the Schrödinger equation (in cylindrical coordinates):

$$\frac{\hbar^2}{2M}\left(\frac{d^2}{d\rho^2}+\frac{1}{\rho}\frac{d}{d\rho}+\frac{1}{\rho^2}\frac{d^2}{d\varphi^2}\right)\Psi(\rho,\varphi)$$

$$-\gamma\frac{\mu_0 I}{2\pi r}\mathbf{F}\cdot\hat{\mathbf{e}}_\varphi\Psi(\rho,\varphi)=E\Psi(\rho,\varphi). \tag{10}$$

One can easily verify that $J_z = -\mathrm{i}\,(d/d\varphi) + F_z$, the z-component of the total angular momentum **J**, commutes with H and, therefore, is a conserved quantity.

The quantum problem of a spin 1/2 neutron in the field of a current-carrying wire was first discussed by Vladimirskii [10]. Exact solution for a spin 1/2 problem were obtained by Voronin [17] and Blümel and Dietrich [18]. They obtain a hydrogen-like energy spectrum with energy eigenvalues:

$$E_n = -E_0\frac{1}{(n+\nu+\frac{1}{2})^2}, \tag{11}$$

where ν is the quantum number characterizing J_z. $\nu = \pm\frac{1}{2}, \pm\frac{3}{2}, \pm\frac{5}{2}\cdots$ is a half-integer for a spin 1/2 neutron. To our knowledge, there is no analytic solution to the Schrödinger equation for higher spins. Nevertheless, numerical solutions have been obtained for spin 1 [18] and higher [19].

1.2.1 Adiabatic approximation. For trapping an atom around a current-carrying wire with a finite radius $r_w > 0$, only those states with the wave function completely outside the wire are interesting. These are the high angular-momentum states where the adiabatic approximation can be applied.

In this case ($l \gg 1$) the atom–current systems look like a two-dimensional hydrogen atom in Rydberg states. The wire resembles the "*nucleus*" and the atom now takes the place of the "*electron*". In the adiabatic approximation, we can determine the energy levels by a semiclassical Bohr-Sommerfeld quantization condition, as given by [11, 20].

$$\oint_{\text{orbit}} P\mathrm{d}X = 2\pi\hbar(n+\tfrac{1}{2}) + \hbar\Phi_{\text{geom}}, \tag{12}$$

where $\Phi_{\text{geom}} = \oint \mathbf{A}_{\text{adiabat}}\,\mathrm{d}x = 2\pi m_F$ is the geometric phase, caused by the parallel transport of the magnetic moment $\mu = \gamma m_F$ along the orbit [11]. This additional geometric phase in the quantization condition (12) results in a shift of the quantum-mechanical energy levels when compared to an electron in a two-dimensional Coulomb potential. The difference can be seen by comparing the exact solutions for a spin 1/2 neutron in a magnetic field of a linear current [17, 18]: $E_n = -E_0/n^2$ to the solution for the two-dimensional hydrogen atom with a spin 1/2 electron [21]: $E_n = -E_0/(n-\frac{1}{2})^2$ (n is an integer in both cases). The energy levels differ by a half-integer quantum number, which corresponds exactly to the additional phase $\Phi_{\text{geom}} = 2\pi\frac{1}{2}$ in (12).

1.3 Typical parameters for trapping an atom with a current

Let us now consider the typical parameter range for which trapping of a neutral atom on a current-carrying wire is possible. We will focus on two different regimes: classical motion of the atom in a Kepler-like orbit, and a microscopic quantum trap in which the total system of the atom and the wire resembles an artificial Rydberg atom in two dimensions. Using the basic relations summarized in Table 1, we calculate typical parameters for trapping neutral atoms on a current-carrying wire in each regime. The

Table 2. Typical parameters for alkali atoms trapped on a current-carrying wire. The upper part of the table gives trapping parameters in the classical regime which is easily reachable with atomic-beam technique. In the second part of the table, we give parameters for microscopic traps resembling a two-dimensional Rydberg atom in its circular states

Atom	Current	Radius [μm]	Binding energy [eV]	l	ω_0	Velocity [cm/s]
Li	2A	100	$1.2\,10^{-7}$	19690	17863	178
Na	2A	100	$1.2\,10^{-7}$	35700	9855	99
Rb	2A	100	$1.2\,10^{-7}$	69000	5096	51
Cs	2A	100	$1.2\,10^{-7}$	85000	4113	41
Li	2.58 mA	2	$7.4\,10^{-9}$	100	226800	45.0
Na	0.79 mA	2	$2.3\,10^{-9}$	100	69030	14.0
Rb	0.21 mA	2	$0.6\,10^{-9}$	100	18462	3.7
Cs	0.14 mA	2	$0.4\,10^{-9}$	100	12028	1.4

values are summarized for various favorite atoms in Table 2.

Our classical example assumes a macroscopic wire of 100 μm diameter that can support currents of 2 A. Typical orbits have $r \approx 200$ μm, and the binding energy is on the order of 10^{-7} eV. A sodium atom in a $m_F = 2$ state in such an orbit has an atomic velocity of approximately 1 m/s, and its orbital angular momentum is on the order of $l \approx 3.5 \times 10^4$.

In the quantum-mechanical example of atoms in circular Rydberg states around the wire, we need to use a mesoscopic wire with a 1 μm diameter which can support a current on the order of mA. A typical orbit with $r = 2$ μm and $l \approx 100$ for a Na atom requires a current of about 800 μA. The binding energy of the sodium atom in a $m_F = 2$ state is then on the order of 2.3×10^{-9} eV. This binding energy has to be compared with the limit for laser cooling of neutral atoms using polarization-gradient cooling, which is on the order of 10 times the recoil energy $E_{rec} = \hbar^2 k^2/2M$ ($E_{rec} = 1 \times 10^{-10}$ eV for a Na atom) [2]. In this regime, the current-carrying wire can be used as a wave guide for matter waves.

1.4 Guiding experiment

Here, we will describe a simple experiment in which a neutral atom is trapped on a current-carrying wire [22]. In the two-dimensional geometry of a straight wire, only the transverse motion is important for a trapping experiment and the longitudinal velocity and the length of the wire only limit the time the atom spends in the trap.

To demonstrate the two-dimensional trapping in the classical region, the transverse motion has to fall within the limits given in Table 2, i.e., typical transverse energies of 10^{-7} eV or transverse velocities on the order of 1 m/s. In a well-collimated atomic beam, with a divergence $< 10^{-3}$ rad, the transverse motion is well within the regime required for trapping in the classical regime ($l \gg 1$).

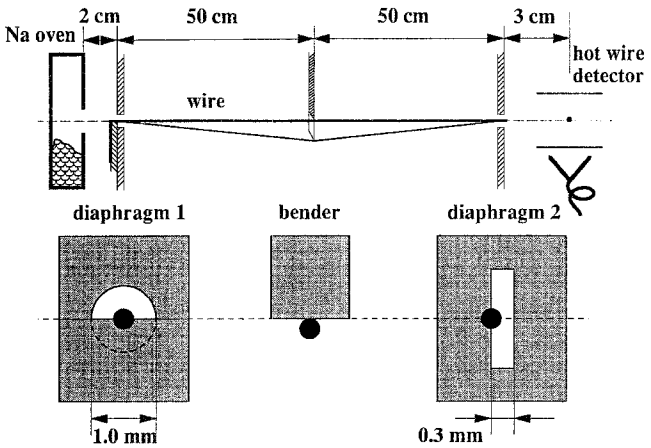

Fig. 3. Basic schematic of the experimental setup. Na atoms are emitted from the oven. The two beam-defining diaphragms hold the wire. The '*wire bender*' and the movable detector are shown. The *inserts* below show in detail the relative geometric arrangement between the apertures and the moveable beam shutter used to bend the wire, and how the wire is mounted

The experiments were performed using an effusive sodium atomic beam with mean velocity of approximately 600 m/s emitted from a 1 mm diameter nozzle of a 100 °C oven. Good collimation was achieved by two apertures spaced 1 m apart (Fig. 3). These apertures were of special shape and also held the 1 m long, 150 μm diameter, W/wire meant to guide the atoms. The apertures were mounted on one long metal rod to guarantee dimensional stability. The whole setup, mounted in the vacuum chamber, was carefully aligned in respect to the source nozzle and the detector with the help of a HeNe-laser beam.

In order to demonstrate the binding of atoms to the wire, a small bend was introduced in the wire ($< 10^{-3}$ rad) to guide atoms along the wire around a beam stop. This was accomplished by a moveable beam blocker halfway between the two collimating apertures. The edge of the beam blocker was parallel to the bottom of the first aperture and perpendicular to the slit of the second collimator (Fig. 3). This beam blocker could be moved into the beam from above, with an accuracy of better than 0.05 mm. Together with the geometry of the first aperture, it blocked the direct beam in a well-defined manner, giving a sharp shadow on the slit of the second aperture. In addition, the blocker bends the wire.

Single sodium atoms were detected using a Re hot-wire detector [23] mounted on a translation stage 3 cm behind the second aperture. By moving the 250 μm diameter hot wire along the slit, the beam profile along the bending direction was measured. For typical operating conditions, the background was on the order of 10 cps with better than a millisecond time resolution.

In the experiment, the position of the wire was first determined by looking as its shadow behind the slit with the beam blocker out of the beam. This defined the reference point of our measurements. As the beam blocker was moved into the beam, its position relative to the wire was determined by its shadow. When the shadow of the beam blocker and the shadow of the wire overlap, the wire starts to bend. The bending angle of the wire could be determined by the position of the shadow of the beam blocker to better than 0.1 mrad. The bending angle could also be determined from reading the micrometer that translates the bender. Both determinations of the bending angle were in good agreement with each other.

A 150 μm diameter W wire can support more than 2A current in vacuum. However, applying such a large constant current heats the wire significantly causing a large thermal expansion, up to a few mm. To compensate for this expansion, the second aperture (it holds the far end of the wire, as shown in Fig. 3) was mounted on a translation stage. A small tension was applied to the wire with a spring to keep it taut.

Even though the wire was kept taut by a spring, the resistive heating of the wire or other mechanical effects on the wire, like magnetic forces, could alter the geometry in the setup. To avoid any systematic changes in the atom flux caused by different alignments with and without the current, and to measure trapping unambiguously, the atom flux was measured alternately with and without current through the wire. Uniform conditions were

achieved by rapidly alternating periods with the current on and with the current off. This was done on a time scale faster than the time constant for the resistive heating or the damping of any mechanical oscillation of the wire, which was on the order of a second.

In a measurement cycle, atoms were counted for time t_{count} (typically 100 ms) with the current off. Then, the current was switched on and a delay of t_{wait} (typically 10 ms) was allowed before atoms were counted again for t_{count}. The current was then switched off again and the time t_{wait} was allowed before starting the counting cycle again. A typical switching time of approximately 100 ms was long compared to the flight time of the atoms along the wire (2 ms) and the detector response time (typically 1 ms). To check for any time-dependent effects on a time scale on the order of the switching time or shorter, experiments were performed over a wide range (one order of magnitude) of parameters t_{coun} and t_{wait}. The experimental results were found to be independent of the times t_{count} and t_{wait} used in the measurement cycle.

The current through the wire was driven by a HP 6825A current power supply and amplifier with a 10 kHz band width and supplied up to 2A constant current. It amplified a square-wave signal generated by the computer controlling the experiment using a digital-to-analog converter. This way, a perfect synchronization of the counting and the current according to the above-described measurement cycle was achieved. The current was measured as a voltage drop across a 1 Ω resistor, using both a fast voltage meter and an oscilloscope. Both current measurements agreed with each other to much better than 10%.

Since other magnetic fields would influence the magnetic trapping of the atoms on the current-carrying wire, all the parts of the experiment were made out of non-magnetic materials: stainless steel, aluminum, and copper. The typical magnetic field generated by 1A at a radius of 200 μm is 10 G, which is much larger than the earth-magnetic field (typically < 0.5 G). No special care was taken to compensate stray fields.

The experiments were performed with various currents up to 2.0 A, for various bends of the wire up to 1.5 mrad. Figure 4 shows a typical experimental run for the detector placed on axis behind the wire. One trace shows the count rate of atoms with the current on and one with the current off. To demonstrate the effect of the current on trapping, the current was switched off completely for the time between 3.5 and 7 s.

The beam profile behind the wire was determined from the detector scans along the exit slit. The data are shown in the left-hand graphs in Fig. 5. The thin line with the symbols is the difference of Na atoms counted with the current on $n(i)$ and the current off $n(0)$. The peak around the wire position (thin vertical line at position 0) is clear evidence of guiding the atoms along the wire and around the bend. The thick dark line shows the fraction of the direct beam reaching the detector. This is the shadow of the bender on the detector plane. One clearly sees the edge moving to increasingly negative positions as the wire is bent.

Monte-Carlo calculations of atoms guided in the magnetic field of the wire were performed using classical dynamics in the adiabatic approximation ($l \gg 1$). The atom enters the first collimating aperture at a random position with a random velocity chosen from the velocity distribution of atoms coming from the effusive source. The internal state of the atom is randomly selected as well as its magnetic quantum number defining the attractive or repulsive nature of the potential $V = -\boldsymbol{\mu}\mathbf{B}$. The atoms then move in Kepler orbits around the wire. The motion along the wire is free up to the bender. At the bend, we

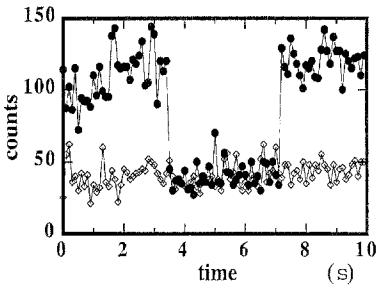

Fig. 4. Raw data from an experiment with 1 A current and a bend of 0.5 mrad. Measurements were done alternatively with the current on for 100 ms (•) and the current off for 100 ms (◇). Between 3.5 and 7.2 s, the current was switched off completely and both count rates agree within the experimental error

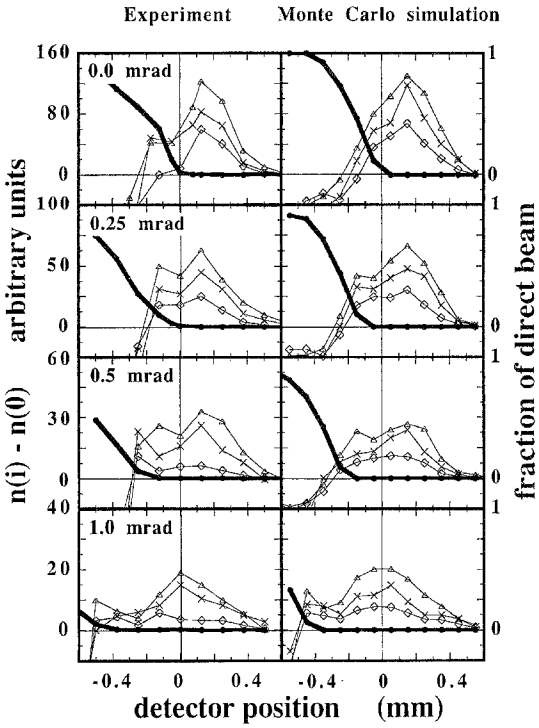

Fig. 5. Na atoms being guided along a 1 m long, 150 μm diameter, W wire (at detector position 0 indicated by the *vertical line*). Experimental data (*left*) and Monte–Carlo simulations (*right*) are shown for a 1.00 mrad bend in the wire. The data are given as the difference $n(i)$–$n(0)$, where $n(i)$ is the number of atoms reaching the detector with current on and $n(0)$ is the number of atoms reaching the detector with current off. The different symbols are for 1.0 A (◇), 1.5 A (×) and 2.0 A (△) current through the wire. The *thick line* shows the fraction of the direct beam reaching the detector. The steep slope shows the shadow cast by the bender

assume a sudden kink in the wire and in the potential. The motion of an atom after the bend is calculated from a new set of orbit parameters obtained by requiring the velocity vector to be the same before and after the bend. From here, they move in new orbits up to the exit slit. Atoms that hit the wire, the bender, or collimators are regarded as absorbed. The Monte-Carlo calculations for the exact parameters (current, wire bend) used in the experiment are shown in the right-hand graphs of Fig. 5. The only free parameter is the normalization. The calculations show good agreement with the experimental data shown in the left-hand graphs. Furthermore, the Monte–Carlo calculations show that atoms, mainly from the low-energy tail of the effusive beam, are guided along the wire.

2 Atom and a charged wire

Consider now the interaction of a neutral atom with a charged wire [25] (Fig. 6). A neutral atom placed in an electric field **E** will acquire an induced electric-dipole moment $\mathbf{d} = \alpha \mathbf{E}$, where α is the electric polarizability of the atom. For simplicity, we will assume α to be scalar, which is true for all alkali-atom ground states. The interaction potential with the electric field is then given by $V_{\text{pol}} = -\alpha E^2/2$. We neglect here all other possible interactions with the electric field [24] like $\frac{1}{c}\boldsymbol{\mu}\cdot(\mathbf{v}\times\mathbf{E})$, which are much smaller.

The electric field of a wire with a finite radius r_w which is held at a potential U relative to a concentric cylinder with radius r_g (Fig. 6) is given by (in Gaussian units):

$$E(r) = \frac{1}{r}\frac{U}{\ln(r_g/r_w)} = \frac{2q}{r}, \tag{13}$$

where q is the charge per unit length on the wire. The relation of the line charge q to the applied potential U is given by the capacitance between the wire and the grounded cylinder. $C = [2\ln(r_g/r_w)]^{-1}$.

The interaction potential of a neutral atom with a charged wire can then be written as:

$$V_{\text{pol}}(r) = -\tfrac{1}{2}\alpha(2q/r)^2. \tag{14}$$

The interaction potential is attractive but, in contrast to the interaction of a magnetic moment and the field of a current-carrying wire (Sect. 1), the potential has the form of $1/r^2$ [25].

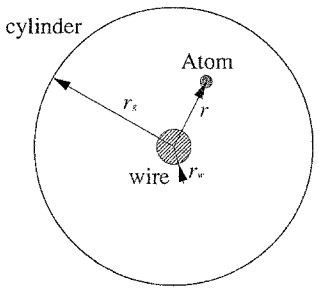

Fig. 6. Geometry for the interaction of a neutral atom with a charged wire of radius r_w surrounded by a grounded cylinder of radius r_g

The attractive $1/r^2$ potential is of special interest [25] because it lies on the border between these $1/r^n$ potentials where the radial motion can be stabilized by angular momentum ($n < 2$), and those where this is not possible ($n > 2$). In three dimensions, this potential has been discussed classically [26] and quantum mechanically [27–30]. The attractive $1/r^2$ has become of more interest lately because the interaction of electrons and ions with the electric dipole of a polar molecule is of this form [31].

The interaction of a neutral atom with a charged wire gives us a realizable two-dimensional model for this peculiar attractive $1/r^2$ potential. In the following paragraphs we will discuss the classical and quantum motion briefly and describe how to make a switch for neutral atoms guided along a wire.

2.1 Classical motion

If the wire is straight, the motion along the wire is free and we can focus again only on the transverse motion. The Hamiltonian for the radial motion is then given by:

$$\mathrm{H}_r = \frac{P_r^2}{2M} + \frac{L^2}{2Mr^2} - \frac{1}{2}\alpha\left(\frac{2q}{r}\right)^2 = \frac{P_r^2}{2M} + \frac{\beta}{r^2}, \tag{15}$$

where the coupling of the effective $1/r^2$ radial potential β is given by:

$$\beta = \frac{L^2}{2M} - 2\alpha q^2. \tag{16}$$

From (16), one can immediately see that there exists a critical angular momentum $L_{\text{crit}} = 2|q|(M\alpha)^{1/2}$, equivalently a critical charge $|q_{\text{crit}}| = L/(4M\alpha)^{1/2}$, so that for $L < L_{\text{crit}}$ ($|q| > |q_{\text{crit}}|$), the total strength β of the effective potential is negative, i.e., the effective potential in the radial equation of motion is attractive. There is no centrifugal barrier like in the magnetic-trapping case. The minimum of the potential is at $r = 0$ and all classical trajectories will go through the center, that is, the atoms will hit the wire. On the other side, for $L > L_{\text{crit}}$ ($|q| < |q_{\text{crit}}|$), β is positive and the effective potential in the radial equation of motion is repulsive, preventing the particle from reaching the center. Trapping an atom in this configuration is also not possible, since the minimum of the potential is at $r = \infty$.

The classical equations of motion in cylindrical coordinates are

$$\frac{d^2}{dt^2}r = -\frac{2\beta}{r^3}.$$

$$\frac{d}{dt}\varphi = \frac{L}{Mr^2}. \tag{17}$$

Integration of the equations of motion gives [15] for the radial motion:

$$r(t) = \sqrt{r_0^2 + \frac{2E_b}{M}t^2 + 2s\sqrt{\frac{2E_b}{M}r_0^2 - \frac{2\beta}{M}}\,t}, \tag{18}$$

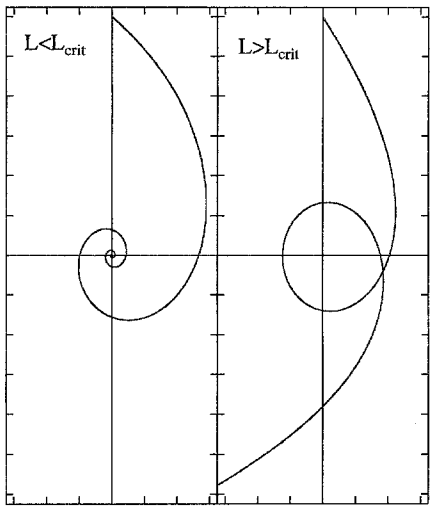

Fig. 7. Classical trajectories of an atom moving in the attractive $1/r^2$ potential of a charged current. The trajectory on the *left-hand side* is for $L < L_{crit}$ and the atom spirals into the center. The trajectory on the *right-hand side* is for $L > L_{crit}$ and corresponds to the atom scattering from a charged wire

and for the motion in φ for $\beta > 0$

$$\varphi(t) = L\sqrt{\frac{M}{2\beta}}\arctan\left(\frac{s\sqrt{r_0^2 - b^2} + \sqrt{\frac{2E_b}{M}}t}{b}\right), \tag{19a}$$

and $\beta < 0$

$$\varphi(t) = L\sqrt{-\frac{M}{2\beta}}\ln\left(\frac{s\sqrt{b^2 - r_0^2} + \sqrt{\frac{-2E_b}{M}}t - b}{s\sqrt{b^2 - r_0^2} + \sqrt{-\frac{2E_b}{M}}t + b}\right). \tag{19b}$$

Here, $b = (\beta/E_b)^{1/2}$ is the point of largest distance (closest approach for $\beta > 0$) to the wire and $s = \pm 1$ depends on the sign of dr/dt at $t = 0$. The time it takes for an atom with $L < L_{crit}$ to fall into the center is given by

$$T_{capture} = \sqrt{-\frac{M}{2E_b}}(s\sqrt{b^2 - r_0^2} + b). \tag{20}$$

Figure 7 shows two trajectories for a particle moving in an attractive $1/r^2$ potential. On the left-hand side, a trajectory resembling the fall into the center for $L < L_{crit}$ is shown. The graph on the right-hand side shows a trajectory for $L > L_{crit}$ coming from infinity and returning to infinity.

Trapping a neutral atom on a charged wire alone is not possible. For a stable two-dimensional trap, the fall into the center has to be stopped by applying an additional strong repulsive potential. This can be achieved by replacing the wire with an optical fiber that is made conducting by a thin metal coating. A charge on the metal coating will bind the atoms. The trajectories are stabilized by the repulsive optical dipole potential of a blue-detuned evanescent wave produced by light in the optical fiber, which will prevent the atom from hitting the fiber [31].

Anotherd possibility to obtain a stable two-dimensional trap was suggested by Hau et al. [25]. They proposed to stabilize the attractive $1/r^2$ potential by oscillating the charge on the wire. The trap is then stabilized by a repulsive ponderomotive force. Hence, trapping neutral atoms in a wire Paul trap should be possible.

2.2 Atom switch

If an atom approaches a charged wire it will fall to the center and hit the wire if its orgbital angular momentum is below the critical angular momentum L_{crit}. The short capture time of atoms in the $1/r^2$ attractive potential of a charged wire allows one to build fast beam shutters for atomic beams. This may be especially interesting in combination with atoms trapped in wave guides like the current-carrying wire.

An electric shutter for a wire guide as described in Sect. 1 may be built by arranging a concentric cylinder around a portion of the wire (Fig. 8). Applying a charge to the cylinder will introduce the additional attractive $1/r^2$ potential and the atom can be captured at the wire. The cylinder has to be long enough so that the traversing time is longer than the capture time. Typical capture times for a guide from Table 2 are given in Table 3.

3 A wire–ring trap for neutral atoms

Even though the static electric field of a charged wire does not offer a possibility to trap atoms on a wire, it nevertheless has some appealing properties that allow modifications to the two-dimensional trapping of a neutral atom on a current-carrying wire, as discussed in Sect. 1.

First, we discuss how the addition of an attractive $1/r^2$ potential, as discussed in Sect. 2, will change the classical dynamics of an atom around the current-carrying wire.

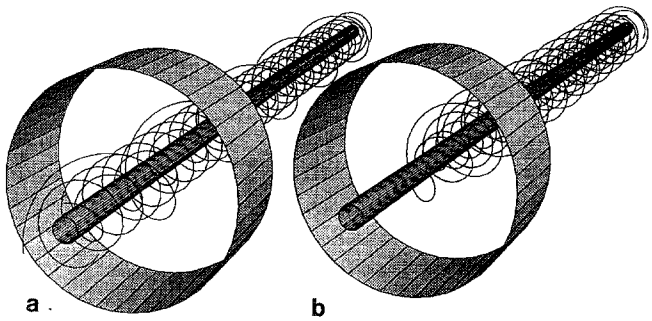

Fig. 8a, b. Proposal for an electric shutter for atoms guided along a current-carrying wire. Sample trajectories for atoms guided along the wire are shown in (**a**). If the cylinder around the wire is held at a potential so that $L < L_{crit}$, the switch will shut the guide and the atoms will spiral to the wire and be absorbed (**b**)

Table 3. Typical parameters for the interaction of alkali atoms with a charged wire. The potentials U are given for a ratio $r_g/r_w = 10^4$, r_w being the radius of the wire and r_g the radius of the surrounding cylinder defining the capacitor. The capture times are given for the orbits given in Table 2 and for an electric potential $U = \sqrt{2}U_{crit}$

Atom	Capturing an atom with $E_b = 1.2\,10^{-7}$ eV, $r = 100$ μm		Capturing an atom with $l = 100$, $r = 2$ μm	
	U_{crit} [V]	T_{capt} [ms]	U_{crit} [V]	T_{capt} [ms]
Li	3700	5	18.8	0.42
Na	3400	10	9.6	1.6
Rb	2415	20	3.5	6.1
Cs	2125	25	2.5	9.3

The most important fact here is that the interaction potential is attractive and has a $1/r^2$ radial dependence which, as pointed out before, has the same functional form as the repulsive angular-momentum potential in the radial equation. It will modify the motion in the following way.

Let us first consider the case where the adiabatic approximation for the dynamics of the magnetic interaction is still valid after the attractive $1/r^2$ potential is added. To keep the effective radial potential the same ($L_{eff} = (2M\beta)^{1/2} = L_{old}$, the orbit will have to have higher angular momentum $L_{new} = (L_{old}^2 + 4M\alpha q^2)^{1/2}$ to compensate for the additional attractive $1/r^2$ potential. In this case, the radial equation will look the same, and therefore the radial motion will be unaffected. The addition of an attractive $1/r^2$ potential will only require a faster φ motion around the wire. The orbits will, in general, not be closed. The effect of a small additional $1/r^2$ potential results in a precession of the orbit with a precession angle given by $\delta\varphi = -4\pi\alpha q^2/L^2$.

In addition to the above described modification of the Kepler problem in the adiabatic approximation, the application of this additional $1/r^2$ potential will change the degree of adiabaticity of the classical orbits. Eventually, by applying larger and larger electric fields, the motion around the wire will speed up to such an extent that the adiabatic approximation will no longer be valid. We can define a characteristic charge q_{char} on the wire when the orbit frequency ω_{orbit} for a circular orbit is equal to the Larmor frequency ω_L. For $q = q_{char}$, the adiabatic approximation brakes down. Assuming $l_{old} \gg m_F$, one finds $q_{char} = l_{old}/m_F\ l_{old}/(4Mc)^{1/2}$. In such a regime, trapping in the high-field seeking state in the non-adiabatic regime can be studied.

3.1 The wire–ring trap

The addition of an electric potential to the two-dimensional trapping configuration of a current-carrying wire has some other appealing possibilities. By shaping the electrode around the wire, one can make the electric field and thus the electric interaction potential of the neutral atom dependent on the position along the wire. In this manner, one can build a three-dimensional high-field seeking trap for neutral atoms using static fields.

The two-dimensional trapping of an atom using a current-carrying wire has the disadvantage that the time the atoms spend in the trap is limited by the velocity of the atom and the length of the wire. Even with long wires and laser-cooled atoms, trapping times much longer than one second would be difficult to achieve. This severely limits the ability to study quantum structure in the motion of an atom around the wire. The possibility to confine the atoms also in the third dimension, along the wire has the clear advantage that the atom stays, in principle, confined to a small controlled trap area. Trapping atoms in a three-dimensional wire trap will be especially important in studying the motion in a combined magnetic and electric field for both the adiabatic and the non-adiabatic regime in more detail. This is essential in studying transitions between quantum levels and investigating possible quantum-statistical effects.

A simple geometry to achieve a three-dimensional trap is the following. Imagine the configuration of a concentric charged ring with radius r_r around the wire at position $z = 0$, as shown in Fig. 9. The electric field for a ring with an outer diameter of 1 mm and an inner diameter of 0.2 mm concentric around a 4 μm diameter wire is shown in Fig. 10. Here, a cylinder with a radius of 1 cm, much larger than the ring diameter, was added in the calculation, to define the boundary conditions for large r. At any line parallel to the z-direction (along the wire), the electric field will be a maximum in the plane of the ring ($z = 0$). The resulting additional interaction potential $V_{pol}(r) = -\alpha E(r)^2/2$, shown in Fig. 11a, has a local minimum at $z = 0$. Close to this minimum, the potential can be approximated by a harmonic

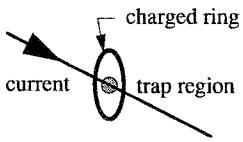

Fig. 9. Arrangements for the atom wire–ring trap. The radial confinement is given by the interaction of the magnetic moment of the atom with the magnetic field of the current in the wire. The trap is closed in axial direction by the electric field of a charged ring

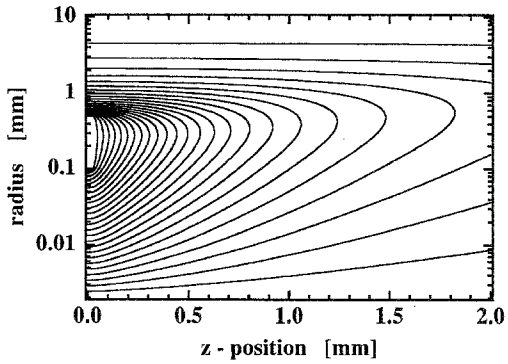

Fig. 10. Electric field in the wire–ring trap. The charged ring has 1 mm outer diameter and a 0.1 mm radius hole and is 0.2 mm thick. It is mounted at $z = 0$, concentric around a 2 μm radius, straight wire at ground potential in the z-direction. The whole setup is mounted inside a 10 mm radius, grounded cylinder. Only the electric field for positive z is shown for this symmetric configuration

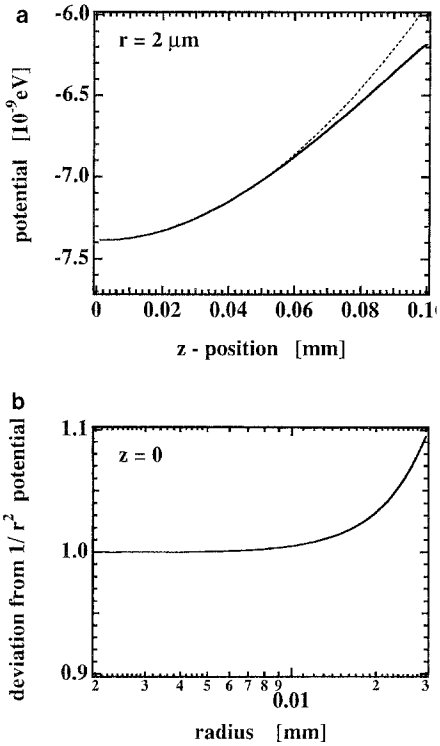

Fig. 11a, b. The interaction potential $V_{pol} = -\alpha E^2/2$ of a Li atom in the wire–ring-trap geometry of Fig. 10. In (**a**) the axial confinement potential for a potential difference of about 9 V between the ring and the wire. The electric interaction potential is of the same order of magnitude as the magnetic interaction of binding a Li atom in a circular Rydberg state with $l = 100$ (Table 2). The *dashed line* is a harmonic-oscillator approximation to the confinement potential close to $z = 0$. (**b**) show the deviation of the radial potential in the plane of the charged ring from the ideal $1/r^2$ form expected from a charged cylinder around the wire. Note that the potential is very close to the $1/r^2$ form up to about 10 μm, that is, 10% of the inner-ring radius

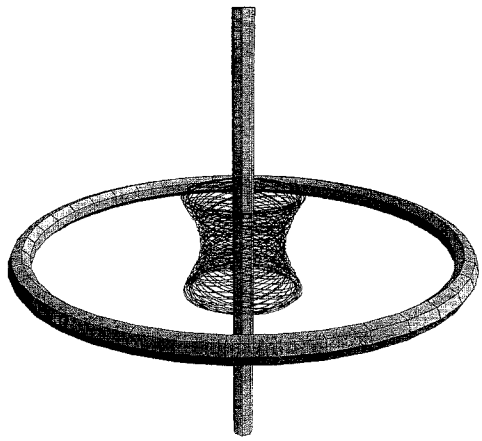

Fig. 12. Classical trajectories of an atom trapped in the wire–ring trap. The trajectory is obtained from numerical integration of the classical equations of motion in the combined electric and magnetic fields of the wire ring. The strength of the electric and magnetic interaction is chosen to be of the same magnitude. The initial position of the atom is in the plane of the ring and the initial velocity is chosen to give a circular motion in the plane of the ring and to have a small additional velocity component along the wire axis. The ring itself is only shown for illustration and is not to scale

oscillator. This local minimum of the electric-interaction potential at $z = 0$ gives longitudinal confinement, and, in combination with the trapping of an atom on a current-carrying wire, a three-dimensional trap for neutral atoms around a wire can be built.

It is also interesting to point out that, close to $z = 0$ ($z \ll r_r$) and for $r \ll r_r$, the radial dependence of the interaction potential $V_{pol}(r) = -\alpha E(r)^2/2$ is close to the $1/r^2$ potential, as expected for a charged cylinder around the wire. In Fig. 11b, one sees clearly that for $r < 30$ μm, the potential on the wire–ring trap is indistinguishable from the $1/r^2$ potential form of an infinitely long cylinder. Therefore, all the implications discussed above for an addition of a charged cylinder to the current trap are to first order also applicable for the charged ring around the wire.

In a typical wire–ring trap, we will assume that the electric and the magnetic interaction are of similar strength. This translates into the requirement that the critical angular momentum $L_{crit} = 2|q|(M\alpha)^{1/2}$ for the attractive $1/r^2$ potential is equal to the orbital angular momentum of our desired orbit in the magnetic trap L_{old}. Combining both potentials, the orbit in the plane of the ring will have to have an angular momentum of $L_{new} = \sqrt{2}L_{old}$ to compensate for the additional attractive $1/r^2$ potential.

Combining the parameters given in Table 2 for the magnetic trapping and in Table 3 for the interaction with the electric field, one finds, for example, that a line charge of about 67 nC/cm will be needed for trapping Li atoms. If we use a 100 μm dimeter wire and a 1 cm inner diameter ring, this translates to an applied voltage of about 1850 V. Such a trap is about 10^{-7} eV deep and would trap Li atoms with velocities of up to a few meters per second. These velocities are easily reachable with standard laser cooling. In such a trap, the motion of the particles will be completely classical. An example of classical trajectories of a neutral atom in such a wire–ring trap are shown in Fig. 12.

For trapping of neutral atoms in a microscopic trap that required quantization of the motion of the atom, we can start from our $l = 100$ Rydberg-atom-like two-dimensional traps shown in the lower part of Table 2. Using a 1 μm radius wire and a ring with an inner diameter of 0.2 mm, one has to apply about 9 V to make the electric interaction of a Li atom equal to the magnetic interaction for trapping on a current-carrying wire. In the wire–ring trap, the circular orbit with radius 2 μm will then have $l = 141$. The trap depth of about 7.4×10^{-9} eV is within the reach of laser cooling of Li atoms. The spacing of the quantum levels for motion along the wire is on the order of kHz.

Having a stable microscopic trap of a neutral atom exhibiting quantized external motion brings a variety of gedanken experiments close to realization. One can see such a trap as being like an *artificial mesoscopic atom*. The trapped atom, itself a microscopic particle, taking the role of the electron, and the macroscopic wire and ring takes the role of the nucleus. One can imagine studying how to drive transitions between the quantum levels and to investigating the effects of the bosonic or fermionic nature of the atoms on transitions between the levels and on the occupation of the levels. A different, but not less interesting, aspects of these traps is the possible combination with the mesoscopic physics [33] of quantum wires and quantum dots.

4 Conclusion

We have given the basic principles of how to trap a neutral atom on a wire. We studied the interactions of a neutral atom with a current-carrying wire and a charged wire. Atoms can be trapped in a two-dimensional trap on a current-carrying wire. They move in classical Kepler-like orbits around the wire. Using mesoscopic wires and cold atoms, a microscopic trap resembling a two-dimensional Rydberg atom can be built. Trapping on a charged wire is not possible because the $1/r^2$ interaction potential of the atom with the charged wire has no stable bound states. Nevertheless, a combination of both interactions allows us to form a three-dimensional trap. Placing a charged ring around a current-carrying wire makes V_{pol} dependent on the position along, there by resulting in longitudinal confinement, a "*wire–ring*" atom cavity. In these traps, the atoms are trapped in the *high–field seeking* state.

Acknowledgements. I would like to thank H. Walther for his continuing interest and encouragement for this work. Special thanks to J. Golovchenko for his invitation to Harvard and the Rowland Institute of Science and to M. Burns, L. Hau, and all the other colleges at the Rowland Institute of Science for numerous discussions, their hospitality and support during the trapping experiments, and H. Batelaan for numerous discussions and critical reading of the manuscript. J.S. is supported by an APART fellowship of the Austrian Academy of Sciences. This work is supported by grant S065-05 of the Austrian Fond zur Förderung der wissenschaftlichen Forschung.

References

1. A good overview is given in H. Demelt: Rev. Mod. Phys. **62**, 521 (1990).
   H. Walther: *Laser Manipulation of Atoms and Ions*, ed. by E. Arimondo, W.D. Phillips, F. Strumia (North-Holland, Amsterdam 1992) p. 569
   R. Blümel, J.M. Chen, E. Peik, W. Quint, W. Schleich, Y.R. Shen, H. Walther: Nature (London) **334**, 309 (1988)
2. E. Arimondo, W.D. Phillips, F. Strumia (eds.): *Laser Manipulation of Atoms and Ions* (North-Holland, Amsterdam 1992) Special issue on *Laser Cooling and Trapping of Atoms*: J. Opt. Soc. Am. B. **6** (Nov. 1989)
3. A good overview is given in W. Paul: Rev. Mod. Phys. **62**, 531 (1990)
4. K. Klueger, K. Moritz, W. Paul, U. Trinks: Nucl. Instrum. Methods **228**, 240 (1985)
5. N. Masuhara, J. Doyle, J. Sandberg, D. Kleppner, T. Greytak, H. Hess, G. Kochanski: Phys. Rev. Lett. **61**, 935 (1988)
6. A. Migdall, J. Prodan, W. Phillips, T. Bergman, H. Metcalf: Phys. Rev. Lett. **54**, 2596 (1985)
   E.A. Cornell, Ch. Monroe, C.E. Wieman: Phys. Rev. Lett. **67**, 2439 (1991)
7. A. Lagendijk, I.F. Silvera, B.J. Verhaar: Phys. Rev. B **33**, 626 (1986)
8. W. Wing: Prog. Quant. Electron. **8**, 181 (1984)
9. W. Ketterle, D. Pritchard: Appl. Phys. B **54**, 403 (1992)
10. V.V. Vladimirskii: Sov. Phys.-JETP **12**, 740 (1961)
11. A. Shapere, F. Wilczek (eds): *Geometric Phases in Physics* (World Scientific, Singapore 1988)
12. Y. Aharonov, A Stern: Phys. Phys. Rev. Lett. **69**, 3593 1992)
    A Stern: Phys. Rev. Lett. **68**, 1022 (1992)
    Y. Aharonov, E. Ben-Reuven, S. Popescu, D. Rohrlide: Phys. Rev. Lett. **65**, 3065 (1990)
    J. Anandan, Y. Aharonov: Phys. Rev. Lett. **65**, 1697 (1990)
13. A. Messiah: *Quantum Mechanics* (de Gruyter, Berlin 1979) Chap. XVII)
14. This is only true if the magnetic field is low enough and one can neglect the internal structure of the atom, i.e., the Zeeman energy has to be much smaller than the hyperfine splitting. This is fulfilled in all the cases discussed here
15. L.D. Landau, E.M. Lifshitz: *Classical Mechanics* (Pergamon, Oxford 1977) Chaps. 14, 15
16. T. Uzer, D. Forrelly, J.A. Milligan, P.L. Raynes, J.P. Skelton: Science **253**, 42 (1991)
17. A.I. Voronin: Phys. Rev. A **43**, 29 (1991)
18. R. Blümel, K. Dietrich: Phys. Rev. A **43**, 22 (1991)
19. A. Scrinzi: Private communications (1994)
20. M. Wilkinson: J. Phys. A **17**, 3459 (1984)
    H. Kratsuji, S. Iida: Prog. Theor. Phys. **74**, 439 (1985)
21. X.L. Yang, H.S. Guo, F.T. Chan, K.W. Wong, W.Y. Ching: Phys. Rev. A **43**, 1186 (1991)
22. J. Schmiedmayer: Phys. Rev. Lett. (1994) (submitted)
23. N. Ramsey: *Molecular Bems* (Oxford Univ. Press. Oxford 1985) p. 37
24. For a review see: M. Wilkins Phys. Rev. A (1994) (submitted)
25. L. Hau, M. Burns, J. Golovchenko: Phys. Rev. A **45**, 6468 (1992)
26. H. Lamb: *Dynamics* (Cambridge Univ. Press, Cambridge 1929)
27. L.D. Landau, E.M. Lifshitz: *Quantum Mechanics* (Pergamon, Oxford 1977) p. 54
28. K.M. Case: Phys. Rev. **80** , 797 (1950)
29. P.M. Morse, H. Feshbach: *Mechods of Theoretical Physics*, Vol. II (McGraw-Hill, New York 1953) p. 1665
30. L. Hau: Private communication
    L. Hau: to be published
31. J.M. Levy-Leblond: Phys. Rev. **153**, 1 (1967)
    C. Desfrancois, B. Baillon, J.P. Sohermann, S.T. Arnold, J.H. Hendrieks, K.H. Bowen: Phys. Rev. Lett. **72**, 48 (1994)
    C. Desfrancois, H. Abdoul-Carime, N. Khelifa, J.P. Schermann: Phys. Rev. Lett. **73**, 2436 (1994)
32. H. Baatelan, R. Abfatterer, S. Wehinger, J. Schmiedmayer: In *Proc. Europ. Quant. Electron. Conf.* (1994) (in press)
33. B. Kramer (ed): *Quantum Coherence in Mesoscopic Systems* NATO ASI Ser. B, Vol. 254 (Plenum, New York 1991)